Liquid-crystal adaptive lenses with modal control

A. F. Naumov and M. Yu. Loktev

Samara Branch, P. N. Lebedev Physical Institute of the Russian Academy of Science, 443011 Samara, Russia

I. R. Guralnik

Department of Physics, Samara State University, 443011 Samara, Russia

G. Vdovin

Department of Electronic Instrumentation, Technical University of Delft, P.O. Box 5031, 2600 GA Delft, The Netherlands

Received February 24, 1998

We report on a novel approach to the realization of nematic liquid-crystal (LC) phase correctors to form spherical and cylindrical wave fronts. A LC cell with a distributed reactive electrical impedance was driven by an ac voltage applied to the cell boundary to yield the desired spatial distribution of the refractive index. The two-dimensional function of the phase delay introduced into the light beam depends on the frequency of the ac control voltage, the geometry of the boundary electrode surrounding the LC cell, and the electrical parameters of the cell. We realized a cylindrical adaptive lens with a clear aperture of 15 mm × 4 mm and a spherical adaptive lens with circular aperture of 6.5 mm. Both devices are capable of focusing collimated light in the range ∞ . . . 0.5 m. © 1998 Optical Society of America

OCIS codes: 010.1080, 160.3710, 220.3620.

Liquid-crystal (LC) phase modulators have a great potential for use as adaptive optics[1] because of their light-transmitting operation, simple control, reliability, low power consumption, and low control voltage. In many applications the correction of low-order aberrations such as of defocus and astigmatism is of primary importance. The adaptive lenses described in Refs. 2–4 and references therein are controlled by arrays of individual electrodes, approximating the wave front by step functions by means of the zonal correction principle. Good approximation to a continuous wavefront profile in these modulators can be achieved only with a large number of discrete control electrodes.

We suggest a novel approach to forming a smooth continuous distribution of the refractive index in a nematic LC layer over the entire aperture of LC cell, realizing a modal control principle.[5] The spatial modulation of the wave front is defined by the geometry of the contacts located at the periphery of the modulator aperture, by the frequency spectrum of the control voltage, and by the electric characteristics of the LC cell. Ultimately we need a single circular contact to control a spherical adaptive lens and two linear equidistant contacts for a cylindrical lens.

Let us consider the LC cell configuration shown in Fig. 1. The LC layer is sandwiched between two transparent plate electrodes deposited upon glass substrates. The distributed resistance of the control electrode is much greater than that of the ground electrode. A control voltage is applied to the contacts deposited at the periphery of the highly resistive electrode. The initial LC layer alignment is determined by the alignment coating, and its thickness is set by dielectric spacers.

When an ac control voltage is applied to the peripheral contacts (Fig. 1) the active impedance of the high-resistance control electrode and the reactive impedance of the capacitor formed by the LC layer sandwiched between the control and ground electrodes form a distributed voltage divider, resulting in a nearly parabolic distribution of the ac voltage over the LC layer. A simplified equivalent circuit corresponding to the situation described is shown in Fig. 1.

Quantitatively the distribution of control voltage U across the LC adaptive lens is described by the

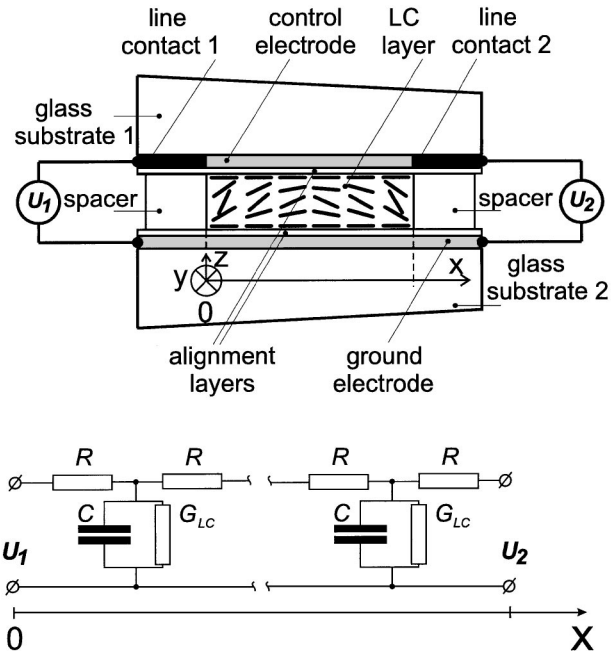

Fig. 1. Top, geometry of the LC cylindrical adaptive lens and bottom, simplified equivalent circuit, illustrating the distributed nature of the reactive impedance of the LC layer sandwiched between high- and low-resistance electrodes.

0146-9592/98/130992-03$15.00/0 © 1998 Optical Society of America

following equation:

$$\nabla^2 U = R_{\square} C_{\square}(U) \frac{\partial U}{\partial t} + R_{\square} G_{\square}(U) U , \quad (1)$$

where

$$C_{\square}(U) = \epsilon_0 \frac{I'}{I'^2 + I''^2}, \qquad G_{\square}(U) = \epsilon_0 \omega \frac{I''}{I'^2 + I''^2}, \quad (2)$$

$$I' = \int_{-d/2}^{d/2} \frac{\epsilon'(\Theta)\mathrm{d}z}{\epsilon'^2(\Theta) + \epsilon''^2(\Theta)},$$

$$I'' = \int_{-d/2}^{d/2} \frac{\epsilon''(\Theta)\mathrm{d}z}{\epsilon'^2(\Theta) + \epsilon''^2(\Theta)}, \quad (3)$$

$$\epsilon' = \epsilon'_{\perp} \cos^2 \Theta + \epsilon'_{\parallel} \sin^2 \Theta ,$$

$$\epsilon'' = \epsilon''_{\perp} \cos^2 \Theta + \epsilon''_{\parallel} \sin^2 \Theta . \quad (4)$$

Here $R_{\square}$ is the sheet resistance of the control electrode; $C_{\square}(U)$ and $G_{\square}(U)$ are the LC specific capacitance and conductance, respectively; ω is the control voltage frequency; S is the clear aperture; $\epsilon'_{\parallel}$, $\epsilon''_{\parallel}$ and $\epsilon'_{\perp}$, $\epsilon''_{\perp}$, respectively, are the real and the imaginary parts of the dielectric constant along and normal to the control electrode; and θ is the LC director deformation angle. The distribution of θ along the z-coordinate can be obtained by solution of the steady-state Ericksen–Leslie[6] equation in an approximation of a uniform electric field across the LC layer:

$$\frac{\partial}{\partial z}\left[(K_{11} \cos^2 \Theta + K_{33} \sin^2 \Theta) \frac{\partial \Theta}{\partial z} \right] - (K_{33} - K_{11}) \sin \Theta \cos \Theta \left(\frac{\partial \Theta}{\partial z} \right)^2 + \frac{(\epsilon'_{\parallel} - \epsilon'_{\perp}) U^2}{4\pi \mathrm{d}^2} \sin \Theta \cos \Theta = 0 , \quad (5)$$

where K_{11} and K_{33}, respectively, represent the splay and bend Frank elastic constants. The approximation is correct when the lens aperture is larger than the LC layer thickness.

The phase delay between ordinary and extraordinary waves is given by

$$\Delta\Phi = \frac{2\pi}{\lambda} \int_{-d/2}^{d/2} \times \left\{ \frac{n_{\parallel} n_{\perp}}{[n_{\perp}^2 \cos^2 \Theta(z) + n_{\parallel}^2 \sin^2 \Theta(z)]^{1/2}} - n_{\perp} \right\} \mathrm{d}z , \quad (6)$$

where $n_{\parallel}$ and $n_{\perp}$ are refractive indices measured along and normal to the LC optical axis.

Figure 2 shows the optimal calculated voltage distribution $U(x)$ and the corresponding distribution of the phase delay $\Delta\Phi(x)$ introduced by the LC layer to a plane-polarized collimated beam transmitted by the device. For phase-only modulation, the polarization of the incident light should coincide with the initial alignment of the LC molecules. Unpolarized light can be treated by two modulators with crossed initial alignment of the LC. The distributions $U(x)$ and $\Delta\Phi(x)$ were obtained for a sine control voltage, $U_1 = U_2 = U \sin(\omega t)$, optimized with respect to the amplitude and frequency. We assumed that the dielectric constants were independent of the frequency, which is justified for nematic LC without dispersion in the frequency range considered. The optical anisotropy of

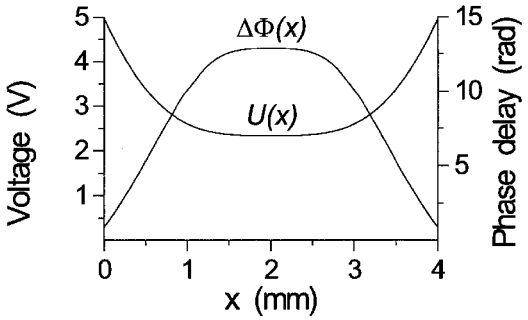

Fig. 2. Control voltage and phase correction across the lens aperture introduced into the transmitted beam.

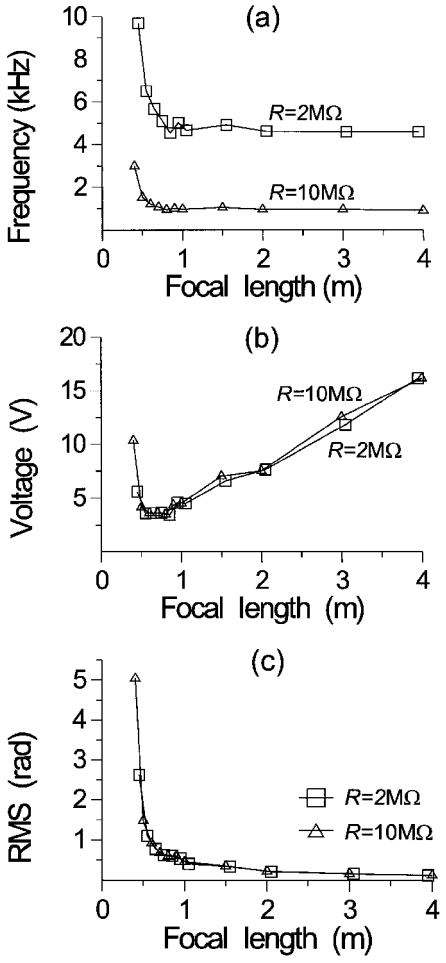

Fig. 3. (a) Control frequency, (b) voltage, and (c) rms error of the parabolic approximation as functions of the focal distance.

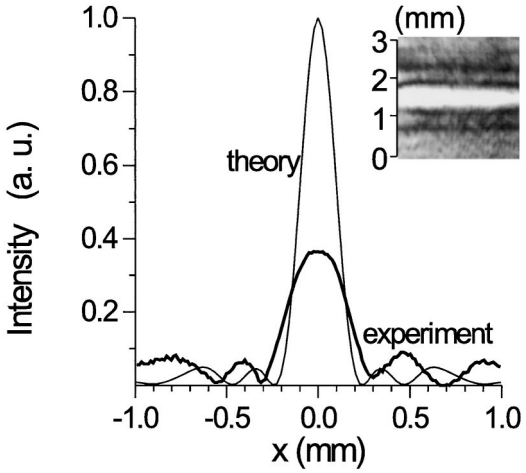

Fig. 4. Comparison of the numerically computed and experimentally obtained focal distributions formed by a cylindrical adaptive lens. The registered intensity distribution is shown in the inset.

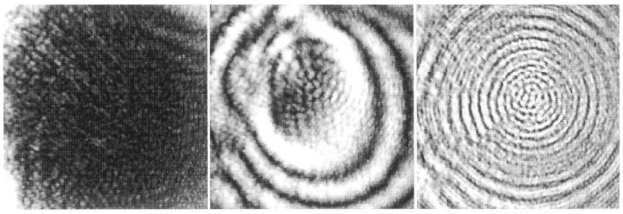

Fig. 5. Interference fringe patterns in a spherical LC lens for control frequencies of 22, 70, and 600 kHz (left to right), observed through crossed polarizers. The spherical adaptive lens has a diameter of 6.5 mm and a LC thickness of 25 μm. The sheet resistance of the control electrode was relatively low, which explains the high working frequencies.

the LC material that we used is 0.224 for $\lambda = 0.66$ μm. In these estimations we used the geometrical parameters of the experimental cell: thickness of the LC layer, 25 μm; distance between linear conductive contacts, 4 mm; aperture area, 0.6 cm^2; resistance between contacts, $R = 2$ MΩ. We assumed the following (experimentally measured) values for dielectric constants: $\epsilon_{\parallel}' = 16.8$, $\epsilon_{\perp}' = 7.14$, $\epsilon_{\parallel}'' = 0.625$, $\epsilon_{\perp}'' = 0.45$, and elastic moduli $K_{11} = 1.2 \times 10^{-12}$ N and $K_{33} = 1.4 \times 10^{-12}$ N.

We used the gradient descent technique to search for optimum control of amplitude and frequency to minimize the rms deviation from an ideal parabolic phase profile. The calculated frequency, voltage, and rms deviation as functions of the focal distance F are shown in Fig. 3. Note that the value of R has almost no effect on the optimum voltage and rms phase error but does affect the optimum frequency range.

As follows from Fig. 3, the rms error of the phase approximation by the LC cell increases with the cell's focusing power. For short focal distances the situation can be somewhat improved by introduction of additional harmonics into the control voltage and further by introduction of phase delays between some of these harmonics.

We assembled modulators with ground plates coated with highly conductive indium tin oxide films. We obtained the best results for high-resistance electrodes by coating glass substrates with titanium oxide films. We selected the deposition regime under which the resistance between 15-mm-long linear highly conductive titanium contacts spaced 4 mm apart stabilized at the level of 2–10 MΩ after a period of coating degradation. The optimal control frequencies for the experimentally fabricated cell were localized in the range of 1...15 kHz, which makes frequency control a rather simple operation and allows for focal distance variation in the range ∞...0.5 m. We visually observed focusing to a distance of 0.5 m but did not estimate the wave-front quality for short focusing distances. Theoretically the phase rms error reaches ~2 rad at a focal distance of 0.5 m for a 4-mm cylindrical lens, which matches the corresponding focal distributions obtained in experiment. The focal line obtained with the fabricated cylindrical lens at a distance of 1.5 m is shown in Fig. 4.

Figure 5 shows the interference between ordinary and extraordinary waves in an adaptive spherical lens with an aperture of 6.5 mm positioned between two crossed polarizers. Resistance R between the center and the circular contact of this sample was relatively low, which explains the high working frequencies. The clearly noticeable asymmetrical aberration was caused by the nonuniformity of the high-resistance control electrode.

The speed of response depends mainly on the rise and decay time constants for the LC layer,[7] which are much larger than the time constant for voltage setting $R_{\square}C_{\square}S$. The speed of LC response depends on the control voltage, which is nonuniform over the cell aperture. Because of this nonuniformity, dynamic phase aberrations are observed during the transition from the off to the on state. Dynamic nonlinearity of response can be used to form dynamically controlled modal phase correctors for a wide spectrum of low-order aberrations.

In this Letter we have reported on our first results with modal control of LC-based adaptive lenses. The performance demonstrated can be further improved by use of more uniform high-resistance substrates and by optimization of the driving parameters. The modal control principle that we have described and implemented is also applicable to multielement LC phase correctors of low-order continuous aberrations.

References

1. J. Gourlay, G. D. Love, P. M. Birch, R. M. Sharples, and A. Purvis, Opt. Commun. **137,** 17 (1997).
2. W. W. Chan and S. T. Kowel, Appl. Opt. **36,** 8958 (1997).
3. N. A. Riza and M. C. DeJule, Opt. Lett. **19,** 1013 (1994).
4. Y. Takaki and H. Ohzu, Opt. Commun. **126,** 123 (1996).
5. R. M. Matic, Proc. SPIE **2120,** 194 (1994).
6. S. T. Wu and C. S. Wu, Appl. Phys. Lett. **53,** 1794 (1988).
7. U. Efron, S. T. Wu, and T. D. Bates, J. Opt. Soc. Am. B **3,** 247 (1986).